Food Control 106 (2019) 106729

Contents lists available at ScienceDirect

Food Control

journal homepage: www.elsevier.com/locate/foodcont

A mathematical model for the prediction of the whey protein fouling mass in a pilot scale plate heat exchanger

Yingying Gu[a], Laurent Bouvier[a], Alberto Tonda[b], Guillaume Delaplace[a,*]

[a] Univ. Lille, CNRS, INRA, ENSCL, UMR 8207 – UMET - Unité Matériaux et Transformations, F-59000, Lille, France
[b] UMR 782 GMPA, INRA, 1 Avenue Brétignières, Thiverval-Grignon, 78850, France

ARTICLE INFO

Keywords:
Dimensional analysis
Thermal treatment
Pasteurization
Whey protein
Fouling deposit
Empirical correlation

ABSTRACT

A better understanding of protein fouling during the thermal treatment of whey protein concentrate (WPC) solutions is critical for better fouling control. In order to understand the impact of various parameters on the total whey protein fouling mass, a dimensional analysis was applied to the experimental data obtained from a pilot scale plate heat exchanger, setting total fouling mass as the target variable. A model was developed to predict the total fouling mass, covering a series of variables including whey protein solution concentration (2.5–25 g/L), calcium concentration (70-120 ppm), running time (90-330 min), fouling solution flow rate (200-500 L/h), total fouling surface area, outlet temperature (82-97 °C) and differences in whey protein concentrate powders. In addition to temperature dimensionless parameters, the main parameters involved in the model are the Reynolds number (2000-5000) and the calcium to β-lactoglobulin molar ratio (2.7–34.7). The model developed concerns only pure whey proteins solutions since all the testing solutions were casein free. This model has allowed us to provide guidelines as to how the above parameters influence fouling within the plate heat exchanger, as well as empirical correlations for predicting such fouling development.

1. Introduction

In the dairy industry, thermal treatment is commonly applied to milk and its derivatives to ensure hygienic safety and to extend shelf-life, or in some cases, to confer specific functions on dairy products for certain applications (cold-set gels, foams and emulsions, encapsulation, as well as films and coatings) (Nicolai, Britten, & Schmitt, 2011). Plate heat exchangers (PHE) have been widely used in the food industry for processing dairy products due to their compactness and flexibility of use (Mota, Carvalho, & Ravagnani, 2015). To guarantee product hygienic safety and long shelf life, thermal treatments such as pasteurization (72 °C during 15 s or 85 °C during 1 s), ultra pasteurization (125 °C-138 °C during 2–4 s), ultra-high-temperature treatment (UHT) (130 °C-145 °C during 1–30 s) are currently applied.

However, protein fouling systematically occurs inside heat exchangers. As is generally known, the formation of the fouling layer has a series of negative consequences including: a decrease in heat exchange rate (Benning et al., 2003; Grijspeerdt, Mortier, De Block, & Van Renterghem, 2004; Jun & Puri, 2005b; Lalande & Tissier, 1985; Mahdi, Mouheb, & Oufer, 2009), an increase in pressure drop, sometimes leading to leakage in the heat exchanger (Benning et al., 2003; Fryer, Christian, & Liu, 2006; Grijspeerdt et al., 2004; Lalande & Tissier, 1985) and risks of further bacterial growth (Dauf in et al., 1987; Fryer et al., 2006; Jun & Puri, 2007). Frequent cleaning of the heat exchanger is thus required, which is undoubtedly time and energy-consuming (Georgiadis, Rotstein, & Macchietto, 1998; René & Lalande, 1988). Cleaning also requires production to be stopped, thereby inducing downtime every day.

These important economic and environmental costs (Zouaghi et al., 2019) associated to fouling explained why scientists have been interested in understanding dairy fouling mechanisms (Bansal & Chen, 2006; Kroslak, Sefcik, & Morbidelli, 2007; Lalande & Tissier, 1985; Sadeghinezhad et al., 2015) for over the last 30 years. The issues of these studies are to predict and control this detrimental phenomenon.

Milk (Boxler, 2015) is almost composed of water (87.5% w/w), fat (3.9% w/w), lactose (4.6% w/w), minerals (0.8% w/w) (calcium, magnesium, sodium, potassium, citrate, chloride, carbonate calcium, phosphate calcium) and proteins (3.4% w/w). Among the proteins, 80% are caseins and 20% are whey proteins composed mainly of β-lactoglobulin and α-lactoalbumin.

Whey Protein solutions are casein-free milk derivatives. The protein content in whey protein concentrate varies from 65 to 75%. Whey protein concentrates are manufactured by the ultrafiltration of whey. To obtain them, whey is passed against a semipermeable membrane,

* Corresponding author.
E-mail address: guillaume.delaplace@inra.fr (G. Delaplace).

https://doi.org/10.1016/j.foodcont.2019.106729
Received 30 August 2018; Received in revised form 20 June 2019; Accepted 21 June 2019
Available online 26 June 2019
0956-7135/

which selectively allows passage of low-molecular-weight materials such as water, ions, and lactose, whilst retaining higher-molecular-weight materials such as protein in the retentate. The retentate is then further concentrated by evaporation and spray-dried to yield whey protein concentrates (WPCs). WPCs are generally available commercially with a protein content of about 35, 50, or 75%. WPC 35% is often considered to be a skim milk powder analog. A WPC with a higher protein content, particularly the 75% product, is generally required by the end user to have defined and reproducible functionality.

Whey protein solutions in dairy manufacture are often elaborated to obtain various milk derivative. In this case, these solutions are obtained after rehydrating whey protein concentrate powders that consists of up to 80% protein by weight. The remaining 20% of the whey concentrate powder contains fats (1%), mineral (2.9%) and lactose (1.1%). Due to the difficulty of storage and avoiding the natural variations of raw milk or whey, whey protein concentrate (WPC) or whey protein isolate (WPI) have been used to obtain reproducible fouling behavior. Researchers have found that, whatever the dairy derivative (milk or whey protein solutions), a whey protein namely β-lactoglobulin (β-lg) plays a key role in fouling formation (Lalande & Tissier, 1985; Blanpain-Avet et al., 2012; Truong, Kirkpatrick, & Anema, 2017). Although β-lg makes up only 10% of raw milk proteins, it can constitute half of the protein deposit content (Lalande & Tissier, 1985; Truong et al., 2017). The fouling formation in the temperature range of 75–100 °C (Belmar-Beiny, Gotham, Paterson, Fryer, & Pritchard, 1993; Burton, 1968; Changani, Belmar-Beiny, & Fryer, 1997; de Jong, 1997; Lyster, 2009) was denoted *type A* and contains mainly proteins. At higher temperatures, the fouling deposit contains fewer proteins but more minerals and is named *type B* fouling. Among inorganic compounds, ionic calcium and calcium phosphate complexes (CaHPO4, $Ca_3(PO3)_2$, etc.) are the most frequent mentioned elements involved in the fouling build-up.

From the different investigations dealing with the formation of fouling deposit, it has also been previously shown that two major destabilizing mechanisms lead to fouling during heat treatment of milk-based products (whey, milk, solutions of inorganic ions together with milk proteins). The former is the formation of activated β-lg molecules due to heat denaturation while the second is precipitation of salts (calcium, calcium phosphate or calcium phosphate-protein/fat complexes) contained in the fouling solution. Salts precipitation and protein denaturation can directly occur onto the hot layer in the vicinity of the stainless steel wall surface or in the bulk, depending to the temperature magnitude in these zones and mineral/protein composition of milk derivative which influence heat denaturation and inverse salt precipitation.

The fact that mineral compound plays a key role and should not be neglected when predicting fouling mass deposit was clearly illustrated by Guérin, R. et al., in 2007 and Khaldi, M. et al., in 2018 (Guérin, Ronse, Bouvier, Debreyne, & Delaplace, 2007; Khaldi, Croguennec, André, Ronse, Jimenez, Bellayer, et al., 2018). These studies have pointed out that the mineral content of the fouling solutions changed both the structure and the fouling rate of a deposit. Recently, analyzing fouling mass deposit data with increasing protein content and fixed calcium content, Khaldi M. et al., in 2018 demonstrated that contrary to what could be expected, the fouling mass is not positively correlated to the protein concentration of the WPC fouling solutions, but can be ranked according to the calcium/protein molar ratio.

Even, not yet fully demystified, an overview of heat-induced fouling mechanisms at molecular level of whey or milk at neutral pH can be schematically given (see Bansal & Chen, 2006; Changani et al., 1997; Daufin et al., 1987). Upon heating, β-lg molecules unfolded, which promoted the exposure of free thiol groups and a progressive increase of the concentration of active β-lg molecules (unfolding species). These active β-lg molecules could be generated either on the thermal layer of the stainless steel wall of the PHE or either in the bulk fluids, depending whether local temperature is higher than denaturation temperature between 65 and 72 °C. These active β-lg molecules sticks on the hot surface to constitute a first fouling layer while the latter forms aggregates in the bulk or contributes to deposit build-up after being transported to the surface. This behavior of β-lg upon thermal treatment at neutral pH has forced authors to assume that β-lg denaturation followed a two-step reaction: unfolding then aggregation (Petit, Herbig, Moreau, & Delaplace, 2011; Tolkach & Kulozik, 2007). Simultaneously, under the temperature increase, calcium complexing substances precipitate calcium salts (mainly calcium phosphate complexes). These solid calcium-based elements and ionic calcium in the derivative milk acts as binding agent and promote interactions between heat denaturated β-lg molecules (β-lg alone or aggregated to β-lg-casein of milk micelles), forming stable co-precipitates with the protein and accelerating the fouling layer growth.

Accordingly, even though a general dairy fouling mechanism can be proposed involving interactions between heat denatured protein and calcium compounds, it appears that fouling mechanisms are strongly different, depending whether the derivative milk-based product (whey, milk and so on) contains casein micelles or not. The presence of casein micelles reduces the opportunities of foulant intermediate (activated β-lg molecules and calcium phosphate) to feed the fouling layer by allowing, on one hand, calcium phosphate to insolubilize in casein micelles (as micellar calcium phosphate) and, on the other hand, enable activated β-lg protein to aggregate on casein micelle surface upon heating.

Note that the mechanism for fouling of dairy derivative during pasteurization at low temperatures is qualitatively understood, but fouling in Ultra-high-temperature treatment is still less so as recently discussed by (Sadeghinezhad et al., 2015).

These results, combined with those of Belmar-Beiny M.T. et al., in 2013 and Petit J. et al., in 2013 (Belmar-Beiny et al., 1993; Petit, Six, Moreau, Ronse, & Delaplace, 2013) illustrating that fouling protein mass obeys a non-linear dependency on temperature, indicate that any prediction of protein fouling mass deposit is not an easy task. The numerous influencing parameters and the non-linear dependency are hurdles to be crossed before establishing a predictive correlation of the fouling mass (Changani et al., 1997).

Mathematical models have been developed by researchers to predict the fouling dynamics in PHE.

From a physical point of view, the deposit growth rate may be regarded as the difference between deposition and removal rates. As suggested by Awad, MM. in 2011 (Awad, 2011), various fouling curves shapes (linear, falling rate or asymptotic fouling curves,..) with or without a lag time can be obtained and depend both on the nature of the physical quantities used for monitoring fouling (thermal resistance, pressure drop, mass of fouling deposit …), the type of dairy derivative (composition..), the process parameters (flow rates and inlet temperatures of processed protein solution and heat medium fluid) and to a certain extent on the duration of the fouling runs. For example, whey protein solutions processed in plate heat exchanger can produce linear fouling curves with a lag time, when the evolution of thermal resistance is plotted against time (Khaldi, Blanpain-Avet, Guérin, Ronse, Bouvier, André, et al., 2015; Khaldi, Ronse, André, Blanpain-Avet, Bouvier, Six, et al., 2015).

Two approaches were mainly used to predict the fouling dynamics in PHE: mechanistic models based on differential mass, energy and reaction balances and Computational Fluid Dynamics (CFD).

Georgiadis, M.C. et al. developed a mechanistic model in 2 dimensional (2D) predicting the fouling behavior within PHE (Georgiadis & Macchietto, 2000). This 2D model was taken up latter as the basis by many authors. This model, comprising a set of partial differential describing mass and heat transfer of a PHE channel, coupled with kinetic models depicting denaturation. Suitable boundary conditions are then imposed to connect the adjoining channels constituting the whole PHE. The change of heat transfer due to fouling was described in terms of dimensionless Biot number, related to a rate model for the deposition of aggregated Protein. As 2D, the model is relatively fast to solve. Model of

this type are capable of describing thermal and hydraulic performance under fouling with good agreement, but the description of the fouling layer (and consequently fouling mass) is limited due to certain simplification hypothesis assumed by the model (aggregates are often considered as the unique fouling source, no influence of calcium content in denaturation and rate of deposit, no re-entrainment of the deposit, no salts precipitation, homogeneous thickness of deposit and no influence of corrugated pattern of the plate..) and difficulty to get experimental data for certain parameters used by the models (deposit density, deposit thermal conductivity, deposit specific heat capacity).

Other studies have simulated the milk fouling process in PHE three-dimensionally, based on hydrodynamic and thermodynamic principles using computational fluid dynamics code (Jun & Puri, 2005a; Bouvier et al., 2014). The design of each plate is simulated and hence reality is much better mimic (effects of detailed geometry and 3 dimensional spatial resolution). However, the computational efforts required is very intensive, requiring simplifying assumptions are made (turbulency model, decoupling thermal and hydraulic aspect, single 2D channel and pseudo-steady sate approach with fixed time steps such in Pan, Chen, Mercadé-Prieto, & Xiao, 2019. Similarly to 2D mechanistic model, CFD also required more realistic/experimental data for certain inlet parameters of the model (deposit density, deposit thermal conductivity, deposit specific heat capacity). In the same way, more sophisticated kinetic models for reflecting β-lg denaturation and for describing how varying fouling source (unfolded, aggregated species and calcium-based complex) contributes to deposit build-up after getting in contact with the fouling layer or the hot wall, are required. These knowledge-based model are missing and results delivered by CFD depends on their accuracy. For all these reasons, even if reality is much better mimic (effects of detailed geometry and 3D map of temperature and velocities distribution), we are still far from being able to use CFD.

A conclusion from the above analysis is that, the modelling of fouling phenomenon is very intricate. However, mechanistic and CFD models are ongoing and in progress, even if they presently fail to accurately predict fouling mass of deposit since the underlying mechanisms occurring in fouling phenomena are not fully understood and consequently cannot be mathematically described in their integrality. Most of modelling approaches concerning fouling of whey protein solutions were based, by considering β-lg protein deposition only and putting aside the contributions of calcium species.

Beyond those pioneer works investigating fouling in PHE, a lot of experimental fouling data of mass deposit are available, especially for whey protein solutions. Unfortunately, experimental data concerning fouling runs were often obtained with varying operating conditions. Indeed, some of them were performed either at a constant product flow rate, a constant product outlet temperature, or for a single type of whey powder concentrate, a fixed number of channels or fixed mineral contents (Blanpain-Avet, André, Khaldi, Bouvier, Petit, Six, et al., 2016; Fryer et al., 1996; Khaldi et al., 2015; Lalande & Tissier, 1985; Petit et al., 2013). Consequently, it is very difficult to obtain a precise view of the key influencing physical quantities from the analysis of these individual series, rendering their use in predicting the outcomes of other processing conditions perilous. The current work is in line with this question and propose to set a fouling model of deposit mass for varying whey protein concentrates (WPC) heat treated in different operating conditions. These experimental data were all obtained by our group and gathered in a database.

Dimensional analysis (DA) is a powerful approach for modelling processes when full and exact descriptions of the physical and chemical processes (denaturation of protein species, salt role in fouling mechanisms, transport and adhesion onto surface,..) taking place in a plate heat exchanger are not available, as in the case of fouling phenomena (Delaplace, Loubiere, Ducept, & Jeantet, 2015). The principle of DA is to establish a set of dimensionless numbers representing influencing and target parameters and then use experimental data for determining the relationship between them. The added value of DA is that grouping dimensional variables into a set of dimensionless numbers allows a reduction in the number of measurements required to describe the system. The DA is mathematically founded and is based on π-theorem (Buckingham, 1914). The π-theorem states that a mechanism characterized by x physical parameters expressible in terms of y independent fundamental quantities i.e. units, can be described by a set of x-y dimensionless numbers. Consequently, the number of dimensionless groups, which fully describe the physical process, is much smaller than the number of dimensional physical quantities. Hence, the set of dimensionless groups obtained represents a synthetic and pertinent dashboard, showing the commands responsible for the evolution of the system and thereby facilitating the identification of the process relationships between fouling mass deposit and other influencing parameters. DA is also a help for implementing scale-up of heat transfer in a scientific way.

DA is indeed a powerful tool, relatively easy to implement, which has proved its efficiency in linking operating conditions to product characteristics or performances of the equipment in various food processes as illustrated in (Delaplace, Loubiere, Ducept, & Jeantet, 2015).

In this work, DA was performed, to set the basis of a general model, by predicting the total protein fouling mass in a PHE for different whey powders at various product flow rates, processing times, calcium concentrations and temperature profiles.

2. Material and methods

2.1. WPC fouling solutions

The WPC fouling solutions (corresponding to fouling runs FR1 to FR38) were obtained by rehydrating three types of WPC powders (P1 to P3) supplied by different manufacturers, and then adjusting the amount of calcium.

Fouling trials have been run by our group at INRA over several years. The methods of adjusting the calcium content of the reconstituted whey protein concentrate solution has varied over the years.

Precisely, two methods have been used to adjust the calcium content in the fouling solutions of WPC. Method 1 for powder P1 is where the desired amount of calcium was obtained by mixing different proportions of tap water from Lille (France) and soft water (provided by a water softener -HI-FLO 1, Culligan, Purolite C100E resin, France).

In this case, the calcium content in the soft water, tap water and powders had been previously measured by atomic absorption spectrophotometry with a Spectro AA 55B apparatus (Varian, Palo Alto, CA, USA). The calcium and sodium contents of tap water, varied within a range of 170–200 and 44–64 mg/l, respectively. The range of calcium and sodium contents of the soft water were 1.0–3.0 and 304–341 mg/l, respectively. Before the addition of protein powder, the electrical conductivity of the water mixture (Tap + Soft) varied from 0.113 to 0.116 S/m at 20 °C for calcium concentrations varying from 35 to 55 mg/l.

Method 2 for powders P2 & P3 consisted in obtaining the desired amount of calcium by adding varying amounts of calcium chloride (anhydrous, 96%, Acros Organics, Thermo Fisher Scientific, Waltham, MA, USA). In this case, reverse osmosis water was used in the rehydration step. Reverse osmosis (RO) systems allows a reduction in the levels of total dissolved solids and suspended particles within water. These systems remove a variety of ions (calcium, sodium) and metals as well as certain organic, inorganic and bacterial contaminants. The electrical conductivity of the RO water was measured as 0.0016 μS/m at 20 °C.

The composition of the powders and fouling solutions of WPC and operating conditions are listed in Tables 1 and 2. In comparison with the average cow milk composition (Boxler, C., 2015), fouling solutions of WPC contains a similar amount of whey proteins, varying from 0.2 to 2% w/w (the value is on average 0.6% w/w in milk).

Table 1
Composition of WPC powders according to manufacturers' specifications (P1: PROMILK 852 FB1, IDI SAS-France; P2: PROTARMOR 750, Armor Proteines-France; P3: PROLACTA 95, Lactalis-France).

Powder reference	P1	P2	P3
Total protein (% dry basis)	86.0	80.8	≥95.0
Total protein (%)	80.1	76.0	≥ 90.0
β-lg (% of protein)	66.0	63.0	60.6
α-la (% of protein)	13.3	11.0	-
Fat (%)	1	3.7	≤0.4
Lactose (%)	11	10	≤3.0
Minerals (%)	2.9	4	≤3.0
Moisture (%)	5	5.5	≤6.0

2.2. Fouling runs and determination of the total fouling deposit mass

All the fouling experiments (FR1 – FR38) were carried out by our group, in the same pilot plant (Fig. 1).

FR32-FR38 are recently obtained, unpublished data, while FR1-FR31 belongs to our data base and have already been reported separately by our group in different publications (Blanpain-Avet et al., 2016; Guérin et al., 2007; Khaldi et al., 2015, 2018; Petit et al., 2013). The main aim of these articles was to show: i) that calcium content impacts fouling kinetics for different whey powders ii) that the structure of deposit and denaturation constant are also functions of both calcium and protein composition iii) that temperature profile is also a key parameter, governing unfolding and aggregation of protein species.

In all these studies, the fouling rig was systematically composed of two distinct zones: (i) a preheating zone and (ii) a heating zone composed of a PHE (Vicarb, model V7, Alfa Laval, France), the plates of which were dried and weighed after each fouling run to determine the total fouling deposit mass. The PHE constituting the heating zone was always one channel-per-pass and installed in a countercurrent configuration to optimize the heat transfer. The projected heat transfer area per plate was approximately 0.074 m^2 (0.495 m long and 0.15 m wide). The average space between two plates was 0.0039 m. The heat exchanger arrangement in the preheating zone was not always the same for all the fouling runs. The Actijoule system (Actini, Evian, France, an electric tubular heat exchanger) was used for preheating fouling solutions prepared with powder P3, while a PHE constituted the preheating zone for P1 and P2 powders.

The total fouling deposit mass for each fouling run is given in Table 2. The extent of fouling was determined from the total weight of dry deposits. For that, heat exchanger plates were weighed before each

Table 2
Protein and calcium contents of whey protein fouling solutions, other operating conditions of the fouling runs and calcium adjusting method number.

Fouling solution number	Powder used	Fouling solution concentration	Calcium concentration	Calcium/β-lg molar ratio	Fouling solution flow rate	Fouling run duration	Total fouling mass
		(g powder/L)	(mg/Kg)		L/h	min	kg
FR1	P1 (method 1)	10	100.0	8.67	300.0	120	0.1047
FR2		10	100.0	8.67	300.0	120	0.1530
FR3		10	100.0	8.67	300.0	120	0.1130
FR4		10	100.0	8.67	300.0	120	0.1733
FR5		10	100.0	8.67	300.0	120	0.3773
FR6		10	120.0	10.40	300.0	120	0.1541
FR7		10	120.0	10.40	300.0	120	0.1614
FR8		10	120.0	10.40	300.0	120	0.1550
FR9		2.5	100.0	34.66	300.0	120	0.1352
FR10		5	100.0	17.33	300.0	120	0.1556
FR11		20	100.0	4.33	300.0	120	0.0484
FR12		25	100.0	3.47	300.0	120	0.0290
FR13	P2 (method 2)	10	72.9	6.97	202.0	330	0.2142
FR14		10	79.8	7.64	202.3	330	0.3600
FR15		10	82.2	7.86	203.5	330	0.5090
FR16		10	85.6	8.19	206.4	330	0.5942
FR17		10	70.0	6.70	337.2	330	0.3673
FR18		10	76.3	7.30	324.2	330	0.6861
FR19		10	78.0	7.46	322.4	330	0.6976
FR20		10	86.5	8.28	324.9	330	0.9218
FR21		10	74.6	7.14	499.4	330	0.3242
FR22		10	77.4	7.41	493.8	330	0.3682
FR23		10	77.8	7.44	492.8	330	0.4261
FR24		10	87.4	8.36	495.6	330	0.7141
FR25	P3 (method 2)	10	33.0	2.77	300.0	120	0
FR26		10	95.0	7.99	300.0	120	0.0964
FR27		5	77.0	12.94	300.0	120	0.1143
FR28		5	98.0	16.48	300.0	120	0.2759
FR29		5	104.9	17.64	300.0	120	0.2305
FR30		5	94.4	15.87	300.0	120	0.2118
FR31		5	99.7	16.76	300.0	120	0.2214
FR32	P1 (method 1)	10	98.0	8.49	300.0	120	0.0951
FR33		10	96.0	8.32	300.0	90	0.1013
FR34		10	96.0	8.32	300.0	90	0.1046
FR35		10	97.0	8.41	300.0	90	0.0572
FR36		10	97.0	8.41	300.0	90	0.0735
FR37		10	101.6	8.80	300.0	90	0.0825
FR38		10	101.6	8.80	300.0	90	0.0738

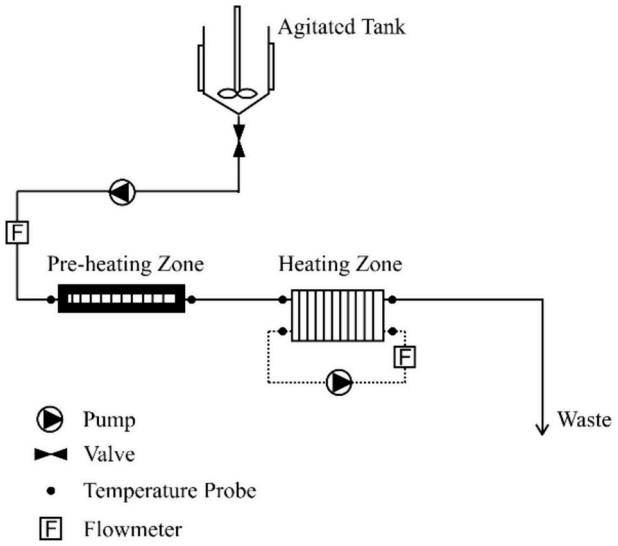

Fig. 1. Schematic diagram of the experimental set-up for fouling runs.

fouling run. Fouled plates were weighed at ambient temperature after being dried in an air oven at 50 °C, and the dry deposit mass on each plate was deduced by subtraction.

Operating conditions for all the fouling runs (i.e. fouling solution concentration and its flow rate, calcium content, the duration of the fouling runs) are given in Table 2. The flow rate was only altered for powder 2 (WPC80), but results will be generalized for all powders later on. Temperature profiles in the different channels of the plate heat exchangers are reported Table 3.

The temperature profiles in Table 3 were obtained by Sphere software, previously developed and patented by our INRA unit. This numerically simulates the temperatures of hot and fouling fluids in all passes based on the knowledge of inlet temperatures and flow rates of the fouling solutions and the hot water, plate properties, and heat exchanger configuration. Sphere Software has been extensively validated in the past by local temperature measurements using sensors installed in PHE. For this work, further validations were carried out to check that the average outlet temperatures of the PHE were accurately predicted. During fouling experiments, the inlet hot water was adjusted to ensure a desired outlet product temperature, varying from 85 °C to 97 °C and corresponding to the outlet product temperature at pass n as indicated in Table 3. The inlet conditions of the hot water and the product at the boundaries of the plate heat exchanger determined the product temperature profile along the PHE.

Finally, Tables 2 and 3 represent 38 independent experiments which have been gathered together and will be analyzed to determine whether any generic process relationship between the dimensionless numbers, thereby relating the causes to the deposit fouling mass of whey protein solutions, could be obtained.

2.3. Key resource table

Resource	Source	Identifier
Chemical		
calcium		
calcium chloride		
sodium		
ProteinPeptide		
whey protein		

3. Results and discussion

In the above section, the recommended procedure for the DA proposed in (Delaplace, Loubière, Ducept, & Jeantet, 2015) was implemented, taking total protein fouling mass in the plate heat exchanger as target variable.

3.1. Influencing parameters for protein fouling in the PHE: relevant list of physical variables

The target variable is the total fouling mass in the PHE (M_f). The relevant physical quantities (influencing parameters) can be classified in three categories (Table 4):

- Product parameters that take into account the composition of the WPC powders and the physicochemical properties of the fouling solutions. Since β-lg plays a key role in type A fouling formation in the temperature range studied (Bylund, 1995, pp. 1–7; Delplace, Leuliet, & Tissier, 1994; Gotham, Fryer, & Pritchard, 1992; Lalande & Tissier, 1985; Lyster, 1970), the weight percentage of β-lg in total protein, %βlg, was chosen as one of the key product parameters. As shown in Khaldi et al. (2018), mineral concentration, mainly the ratio of calcium molar concentration to β-lg concentration, impacts fouling growth. Hence, this variable, $\frac{Ca}{\beta lg}$, was also listed. Since the concentrations of the fouling solutions were very low, the physical properties of water were used to describe the density ρ and viscosity μ of fouling solutions and to calculate the average Reynolds number along the PHE. These approximations were previously adopted and verified by (Delplace, Leuliet, & Leviex, 1997) and (Petit et al., 2013).

The aggregation temperature θ_{agg} and the unfolding temperature θ_{unf} of the fouling solutions were also introduced. These are key variables characterizing the chemical denaturation behavior of β-lg at molecular scale under thermal treatment and exerting an impact on the underlying fouling mechanisms. θ_{unf} corresponds to the temperature on which the unfolding of β-lg's protein starts, due to the denaturation reaction when subjected to thermal treatment. θ_{agg} is the point of transition between two regions: at temperatures below θ_{agg}, unfolding is the limiting step of denaturation reaction, while at temperatures above θ_{agg}, aggregation becomes its limiting step. For practical aspects, θ_{agg} can be experimentally determined by plotting an Arrhenius graph of the protein solutions (Khaldi et al., 2015) as shown by (Tolkach & Kulozik, 2007). The θ_{agg} of the fouling solutions studied were experimentally determined and found to fall between 79 and 81 °C (Petit et al., 2011; Blanpain-Avet et al., 2016; Khaldi et al., 2018). As our goal was to develop an easy-to-use general model, θ_{agg} was herein considered constant, i.e. 80 °C. The unfolding temperature θ_{unf} should be introduced to situate the temperature profile in the PHE relative to the starting of the denaturation reaction, which is the destabilizing phenomena preceding fouling formation. The unfolding of β-lg begins at around 60 °C at neutral pH (Kroslak et al., 2007). Petit et al. (2011) and Khaldi, Blanpain-Avet, et al. (2015) and Khaldi, Ronse, et al. (2015) confirm this unfolding temperature for the whey protein solutions tested, so a constant unfolding temperature of 60 °C was set for the model.

- Process parameters defining the fouling run. The process parameters involved were the velocity of fouling solutions (v), the total amount of protein passing through the heat exchanger (M_{pr}) and the temperature profiles that WPC solutions experienced. M_{pr} is the product of total protein percentage in the powder as given in Table 1, the fouling solution concentrations, fouling run durations and flow rates of the fouling solutions as given in Table 2.

To approximate the temperature profiles, both the first pass and the last pass (θ_{1p}, θ_{op}) outlet temperatures of the WPC solutions were needed, as well as the coordinate of an intermediate point, belonging to

Table 3
Number of passes and temperature profiles in the PHE for the fouling runs.

Number of fouling solutions	Number of passes	Fouling solution temperature at different positions of the heat exchanger (°C)*										
		T0	T1	T2	T3	T4	T5	T6	T7	T8	T9	T10
FR1	5	65	67	71	76	81	84	-	-	-	-	-
FR2	5	65	68	74	79	82	84	-	-	-		-
FR3	5	65	66	68	72	77	83	-	-	-	-	-
FR4	10	65	66	69	71	73	75	77	79	81	83	85
FR5	10	65	68	73	77	79	81	82	83	84	85	85
FR6	5	65	67	71	76	81	84	-		- -	-	-
FR7	5	65	68	74	79	82	84	-	-	-	-	-
FR8	5	65	66	68	72	77	83	-	-	-	-	-
FR9	5	65	67	71	76	81	84	-				
FR10	5	65	67	71	76	81	84	-				
FR11	5	65	67	71	76	81	84	-				
FR12	5	65	67	71	76	81	84	-				
FR13	6	62.3	67.7	74.1	79.3	85.6	91.2	96.8				
FR14	6	60.0	65.3	72.4	77.7	83.9	89.7	96.5				
FR15	6	61.5	67.0	73.2	78.8	85.3	90.7	97.1				
FR16	6	60.4	66.2	72.9	78.0	84.6	90.3	95.8				
FR17	6	63.8	68.1	74.4	79.4	84.5	90.1	95.4				
FR18	6	61.3	65.0	72.3	78.2	83.3	89.4	95.7				
FR19	6	62.6	65.7	72.6	78.4	83.5	89.5	95.0				
FR20	6	62.7	66.2	72.2	77.6	83.1	88.6	94.6				
FR21	6	60.8	66.0	72.6	77.7	83.9	89.5	95.4	-	-	-	-
FR22	6	61.3	66.5	73.2	78.3	84.6	90.2	96.2	-	-	-	-
FR23	6	63.2	68.4	74.1	79.0	84.0	89.9	95.4	-	-	-	-
FR24	6	61.1	66.5	72.9	78.1	84.4	89.9	95.9	-	-	-	-
FR25	10	60.0	63.2	65.7	68.3	70.9	73.4	76	78.7	81.3	84.1	85.2
FR26	10	60.0	63.2	65.7	68.3	70.9	73.4	76	78.7	81.3	84.1	85.2
FR27	10	60.0	63.2	65.7	68.3	70.9	73.4	76	78.7	81.3	84.1	85.2
FR28	10	60.0	63.2	65.7	68.3	70.9	73.4	76	78.7	81.3	84.1	85.2
FR29	10	60.0	63.2	65.7	68.3	70.9	73.4	76	78.7	81.3	84.1	85.2
FR30	10	60.0	63.2	65.7	68.3	70.9	73.4	76	78.7	81.3	84.1	85.2
FR31	10	60.0	63.2	65.7	68.3	70.9	73.4	76	78.7	81.3	84.1	85.2
FR32	5	65.0	68.5	73.2	77.9	83.0	85.0	-	-	-	-	-
FR33	5	65.0	68.5	73.2	77.9	83.0	85.0	-	-	-	-	-
FR34	5	65.0	70.8	75.2	78.5	81.0	82.0	-	-	-	-	-
FR35	5	65.0	70.8	75.2	78.5	81.0	82.0	-	-	-	-	-
FR36	5	65.0	70.8	75.2	78.5	81.0	82.0	-	-	-	-	-
FR37	5	65.0	70.8	75.2	78.5	81.0	82.0	-	-	-	-	-
FR38	5	65.0	68	72	76	80.3	82.0	-	-	-	-	-

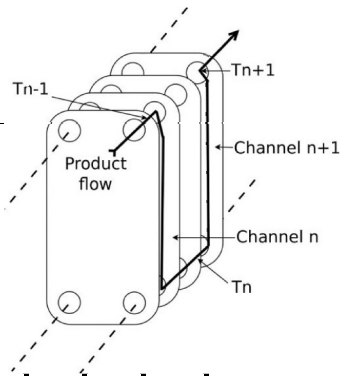

* T0 : product inlet temperature, T1: product temperature at the outlet of the first pass, Tn : product temperature at pass number n outlet and pass number n+1 inlet.

the temperature profile. This approach was adopted to give an approximate description of the temperature profile using a limited number of parameters. The intermediate point was described by two coordinates: n/j and $\theta_{n1} > 80\,^{\circ}C$. n/j is a normalized ratio between 0 and 1 describing the position in heat exchanger of the first pass for which the temperature exceeded 80 °C. j is the total number of passes ($5 \leq j \leq 10$), while n is the channel count with fouling solution temperatures above 80 °C. $\theta_{n1} > 80\,^{\circ}C$ is the outlet temperature of the first pass at a temperature above 80 °C. These two parameters were chosen to define the intermediate point because θ_{agg}, which is around 80 °C, was found to be a transition point between two fouling regimes (increasing fouling mass in sequential channels followed by a maximum plateau) (Khaldi et al., 2018). n/j is used to define how early the maximum plateau was reached.

- Finally, geometrical parameters defining the flow domain and the total fouling surface, delimited by the average space e between 2 plates of the PHE and the total fouling surface $S_{exch} = 2 \cdot j \cdot S$ (with S the surface area of the plate) were also listed.

The target variable and all the relevant physical quantities mentioned above are reported in Table 4.

3.2. Determination of the relevant set of dimensionless numbers

According to the π-theorem, influential dimensional parameters can be grouped into dimensionless numbers through non-dimensionalization based on independent fundamental quantities (i.e. units). In this way, the number of parameters can be significantly reduced (Delaplace et al., 2015; Szirtes, 1998; Zlokarnik, 2002).

The five fundamental units (kg, m, s, °C, mol) involved for the influencing parameters are listed in Table 4. Taking ρ, v, e, [βlg] and θ_{agg}, as repeated variables, the 17 physical quantities, influencing and target parameters, can be converted into 12 dimensionless numbers (Eq. (1)).

Table 4
Influencing and target parameters in the thermal treatment of WPC solutions in the PHE.

Parameter category	Symbol	Name	unit
Target parameter	M_f	total fouling mass	kg
Product	%βlg	weight percentage of β-lg in total protein	-
Parameters	θ_{unf}	starting temperature of β-lg unfolding	°C
	θ_{agg}	temperature above which the denaturation reaction was limited by aggregation of β-lg	°C
	ρ	density of the fouling solution	kg m^{-3}
	μ	dynamic viscosity of the fouling solution	kg m^{-1} s^{-1}
Process parameters	M_{pr}	total protein mass passing through the PHE	kg
	[Ca]	calcium concentration of the fouling solution	mol m^{-3}
	[βlg]	initial β-lg concentration in the fouling solution	mol m^{-3}
	v	flow velocity of the fouling solution	m s^{-1}
	θ_{1p}	fouling solution temperature at the outlet of the first pass	°C
	θ_{op}	outlet temperature of the fouling solution	°C
	n/j	Normalized ratio indicating the position of the channel n, from which the product temperature became above 80 °C (with j as the total number of passes).	-
	$\theta_{n1>80}$	temperature of the first pass that had a temperature above 80 °C	°C
PHE design parameters	e	average space between 2 plates of the PHE	m
	S_{exch}	total exchange surface area	m^2
	S_0	surface area per plate	m^2

After rearranging π_3, π_6 *and* π_{10}, as allowed by the method (Delaplace et al., 2015), the Reynolds number appeared and the final set of dimensionless numbers governing mass deposit were obtained (Eq. (2)).

$$\pi_1 = \frac{M_f}{\rho e^3} = f\left(\pi_2 = \%\beta lg,\ \pi_3 = \frac{\rho ve}{\mu},\ \pi_4 = \frac{M_{pr}}{\rho e^3},\ \pi_5 = \frac{[Ca]}{[\beta lg]},\ \pi_6 = \frac{\theta_{1p}}{\theta_{agg}},\ \pi_7 = \frac{\theta_{op}}{\theta_{agg}},\ \pi_8 = \frac{n}{j},\ \pi_9 = \frac{\theta_{n1>80}}{\theta_{agg}},\ \pi_{10} = \frac{S_{exch}}{e^2},\ \pi_{11} = \frac{S_0}{e^2},\ \pi_{12} = \frac{\theta unf}{\theta_{agg}}\right) \quad (1)$$

$$\pi_1 = \frac{M_f}{\rho e^3} = f\left(\pi_2 = \%\beta lg;\ \pi_3 = Re;\ \pi_4 = \frac{M_{pr}}{\rho e^3};\ \pi_5 = \frac{[Ca]}{[\beta lg]};\ \pi_6 = \frac{\theta_{1p}}{\theta_{unf}};\ \pi_7 = \frac{\theta_{op}}{\theta_{agg}};\ \pi_8 = \frac{n}{j};\ \pi_9 = \frac{\theta_{n1>80}}{\theta_{agg}};\ \pi_{10} = \frac{1}{2}\cdot\frac{\frac{S_{exch}}{e^2}}{\frac{S_0}{e^2}} = \frac{S_{exch}}{2\cdot S_0} = j;\ \pi_{11} = \frac{S_0}{e^2},\ \pi_{12} = \frac{\theta unf}{\theta_{agg}}\right) \quad (2)$$

with

$$Re = 2\cdot\frac{\rho ve}{\mu} = 2\rho Q/\mu w \quad (3)$$

The hydraulic diameter is twice the average space e between 2 PHE plates. Q is the flow rate of the fouling solution. w is the width of the plate.

3.3. Dimensionless process relationships

Process relationship Eq. (4) was developed based on fouling runs FR1 to FR31. As.

$\pi_{11} = \frac{S_0}{e^2}$; $\pi_{12} = \frac{\theta unf}{\theta_{agg}}$ is constant during the fouling runs, this was not retained to identify the process relationship.

$$\frac{M_f}{\rho e^3} = j\cdot\left(\frac{M_{pr}}{\rho e^3}\right)^{1.1}\left[k\left(\frac{\theta_{1p}}{60}\right)^{0.40}\left(\frac{n}{j}\cdot\frac{\theta_{n1>80}}{80}\right)^{0.92}\left(\frac{\theta_{op}}{80}-1\right)^{1.48}\left(\frac{[Ca]}{[\beta lg]}\right)^{1.1}+b\right] \quad (4)$$

In equation (4) k and b are functions of Re and $\%\beta lg$ in order to take into account the influence of hydrodynamics and composition of the WPC powder on the total fouling mass:

$$k = -0.9636069\times10^{-8}\cdot Re^2 + 0.6275151\times10^{-4}\cdot Re - 2.761553704 * \%\beta lg^2 + 3.6108447278\cdot\%\beta lg - 1.246764441 \quad (5)$$

$$b = 0.349643\times10^{-4}\cdot Re^2 + (-0.011866944\cdot\%\beta lg^2 + 0.015023552\cdot\%\beta lg - 0.004777303) * Re + 49.633750741\cdot\%\beta lg^2 - 62.824057582\cdot\%\beta lg + 19.902742408 \quad (6)$$

The valid range of this empirical correlation is: $1.89\times10^4 \le \frac{M_{pr}}{\rho e^3} \le 3.29\times10^5$, $5 \le j \le 10$, $2000 \le Re \le 4942$, $60.6\% \le \%\beta lg \le 66.0\%$, $1.053 \le \frac{\theta_{1p}}{\theta_{unf}} \le 1.19$ $0.3 \le \frac{n}{j} \le 0.7$, $1.00375 \le \frac{\theta_{n1>80}}{\theta_{agg}} \le 1.0700$, $1.025 \le \frac{\theta_{op}}{\theta_{agg}} \le 1.21375$, $2.77 \le \frac{[Ca]}{[\beta lg]} \le 34.66$ *and* $\frac{\theta_{unf}}{\theta_{agg}} = \frac{3}{4}$.

The influences of Re and powder composition on fouling mass were found to be non-monotonic (Khaldi et al., 2015), parameters k and b are hence considered as the product of quadratic functions of Re and $\%\beta lg$. The coefficients and indices were determined through regression to give a minimized sum of relative errors between predicted and experimental mass.

In brief, there is a linear correlation between $\frac{M_f/\rho e^3}{j\cdot(M_{pr}/\rho e^3)^{1.1}}$ and $\left(\frac{\theta_{1p}}{\theta_{unf}}\right)^{0.40}\left(\frac{n}{j}\cdot\frac{\theta_{n1>80}}{\theta_{agg}}\right)^{0.92}\left(\frac{\theta_{op}}{\theta_{agg}}-1\right)^{1.48}\left(\frac{[Ca]}{[\beta lg]}\right)^{1.1}$, while the slope and intercept depend on the fouling side Reynolds number and the WPC powder used.

Fig. 2 shows a relatively close agreement between experimental values and predicted values. In most cases, relative errors are within 25%, the mean relative error is 23% and the coefficient of determination R^2 is 0.92. This is satisfactory with regard to the reproducibility of the pilot-scale experiments. The predicting mass relative error is also represented in Fig. 3. It can be seen from Fig. 3 that the predicted fouling mass relative error equivalent to raw residuals are quite evenly distributed around zero, thus indicating that no bias was introduced by the model. The relative error is high for very low fouling mass. One of the explanations is that the mass measurement is insufficiently precise for low fouling masses, due to weighing imprecision for values lower than 0.1 kg. Consequently, it's better to apply the model when predicted fouling mass is higher than 0.1 kg.

Additional fouling runs (FR32 to FR38) were carried out to verify the process relationship developed. They were made with the expectation of validating and consolidating the model for low experimental fouling mass, as the scatter of the model, established by gathering the results of our data basis, were noticed to be more important for these conditions. The prediction was however satisfactory for experiments with an outlet temperature equals to 85 °C but the model failed to predict fouling mass correctly for outlet temperature equals to 82 °C corresponding to the crosses under experimental fouling mass axes in Fig. 2. The model was adjusted for temperature greater than 85 °C and lower than 97 °C. It's a weakness showing that it's dangerous to extrapolate to data outside the valid range of the model.

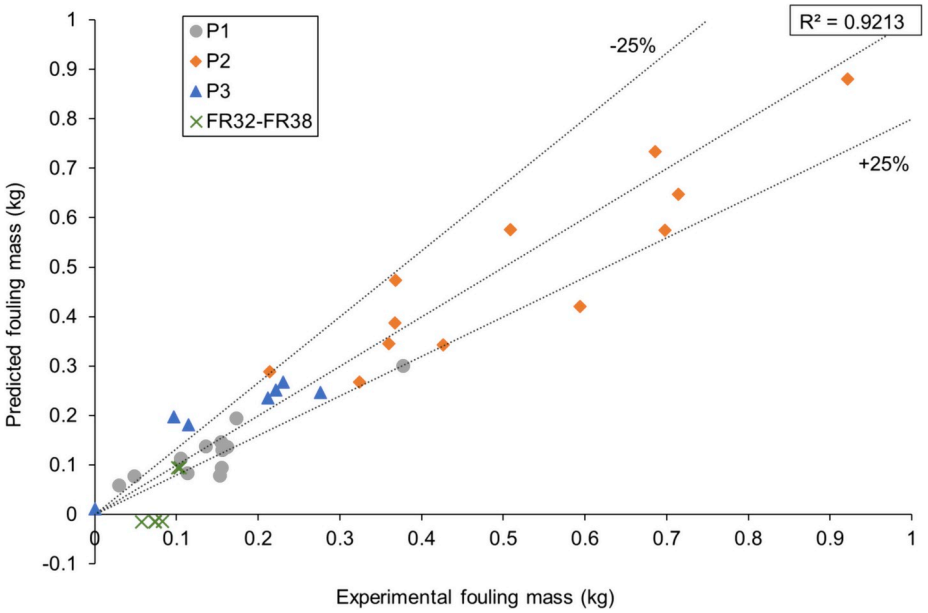

Fig. 2. Predicted and experimental fouling mass in the PHE obtained with powders P1 (dots), P2 (rhombuses), P3 (triangles) and for fouling runs FR32-FR38 (crosses, solutions prepared using powder P1).

3.4. Dimensionless numbers effect on fouling mass

From Eq. (4), it can be seen that the total fouling mass is proportional to the total amount of protein passing through the PHE and number of passes, i.e. the exchange surface. It is also noteworthy that $\frac{M_f / \rho e^3}{j \cdot (M_{pr} / \rho e^3)^{1.1}}$ increases almost linearly with $\frac{[Ca]}{[\beta lg]}$ within the experimental range of this study ($2.77 \leq \frac{[Ca]}{[\beta lg]} \leq 34.66$). This is in agreement with Sherwin and Foegeding (Sherwin & Foegeding, 1997) who state that aggregation of whey proteins is influenced by the $CaCl_2$/protein molar ratio, rather than the concentration of Ca^{2+} or that of protein separately. Khaldi et al. (2018) has recently confirmed that the calcium/protein molar ratio influences β-lg denaturation kinetics and fouling phenomena (Khaldi et al., 2018). Fig. 4 simulates the influence of calcium to β-lg ratio on predicted fouling mass within the 4.5 to 9 range. The linear evolution of the mass deposit with this ratio is clearly shown.

In terms of temperature, the exponent of the inlet, intermediate and outlet temperature parameters of the product $\left(\frac{\theta_{1p}}{\theta_{unf}}\right)$, $\left(\frac{n}{j}.\frac{\theta_{n1>80}}{\theta_{agg}}\right)$ *and* $\left(\frac{\theta_{op}}{\theta_{agg}} - 1\right)$ were respectively 0.4, 0.92 and 1.48. Therefore as expected, within the studied range, the influences of product outlet temperature and the temperature profile (defined by the term $\frac{n}{j}.\frac{\theta_{n1>80}}{\theta_{agg}}$) were much greater than that of the product temperature near the inlet.

The amount of fouling depends on protein deposition rate and its elimination rate from the fouling layer (Szirtes, 1998). As both are functions of Reynolds number, it is logical that the total fouling mass is

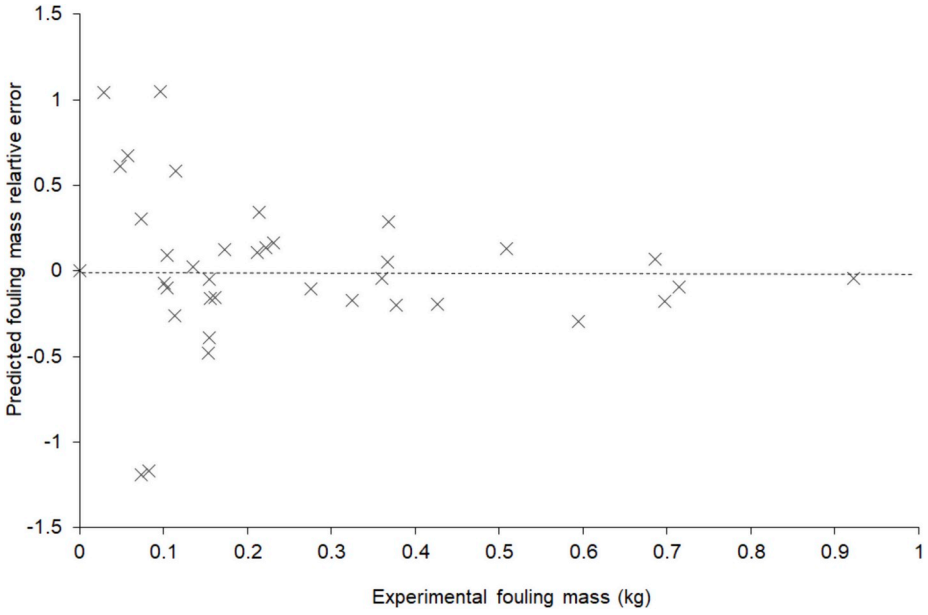

Fig. 3. Predicted fouling mass relative error for experiment fouling runs FR1 to FR38.

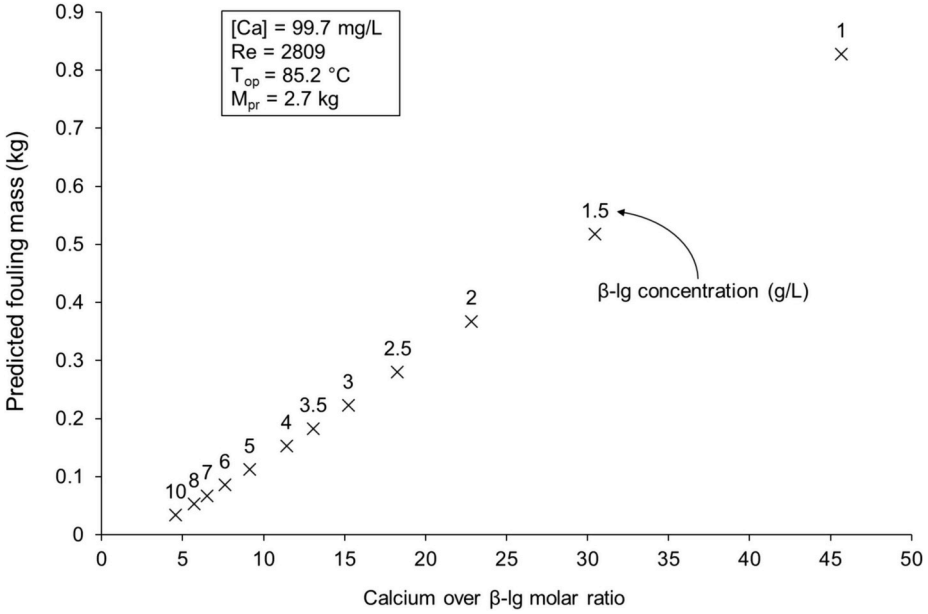

Figure 4. $\frac{[Ca]}{[\beta lg]}$ effect on predicted fouling mass for β-lg concentration varying from 1 to 10 g/L with other parameters fixed at a constant value.

not a monotonic Reynolds function. As for the non-monotonic influence of the $\%\beta lg$ content of the powder, this could be attributed to the fact that β-lg is not the only component involved in the aggregation and fouling process. Although β-lg is the most prominent component involved in the thermal aggregation process, other ingredients such as BSA and α-la are not completely innocent either (Havea, Singh, & Creamer, 2001).

Fig. 5 simulates the effect of the Reynolds number on the predicted fouling mass. The predicted fouling mass increases with the Reynolds number and turbulence intensity until 3500. Between 3500 and 5000, predicted fouling mass decreases. We supposed that this behavior is linked to the heat exchanger plate shape used in this study or some complex physicochemical mechanisms such as attachment and detachment of activated protein. The physico-chemical parameters should be covered by other pi-terms and, hence, can be used to explain the effect on fouling mass.

4. Conclusions

A fouling mass prediction model for the PHE was proposed based on fouling runs with three WPC powders under various conditions through dimensional analysis. The process conditions that were varied include protein and calcium concentration, fouling solution flow rate, running time, number of passes and temperature profiles. After non-dimensionalization, a linear correlation was found between $\frac{M_f / \rho e^3}{j \cdot (M_{pr} / \rho e^3)^{1.1}}$ and $\left(\frac{\theta_{1p}}{\theta_{unf}}\right)^{0.40}\left(\frac{n}{j}.\frac{\theta_{n1>80}}{\theta_{agg}}\right)^{0.92}\left(\frac{\theta_{op}}{\theta_{agg}}-1\right)^{1.48}\left(\frac{[Ca]}{[\beta lg]}\right)^{1.1}$. The protein fouling mass was thus correlated to the total protein mass passing through the PHE, the number of passes, temperature profile, $[Ca]/[\beta lg]$ molar ratio, Re number of the product side and the powder composition ($\%\beta lg$). Within the parameter ranges studied in this work, the fouling mass was found to be nearly proportional to the total protein mass passing through the

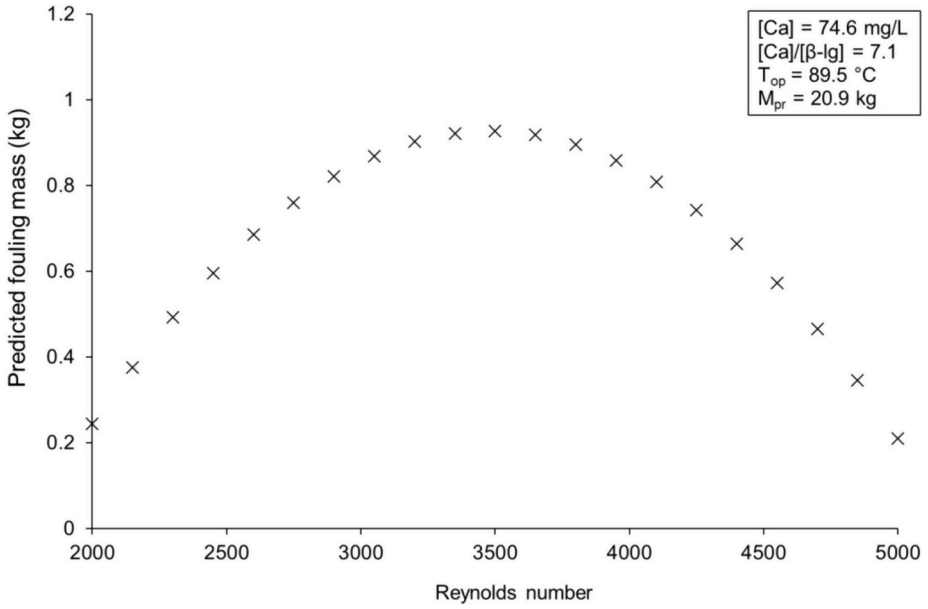

Fig. 5. Effect of Reynolds numbers varying from 2000 to 5000 on predicted fouling mass when other parameters were constant.

PHE and the number of passes, i.e. the total fouling surface, increasing almost linearly with the Ca/ β-lg molar ratio. In order to minimize fouling growth, it is important to control this ratio. For the range of Ca/ β-lg investigated, at a constant calcium concentration, fouling mass decreases if the β-lg concentration increases. The influences of *R*e and powder composition were, however, more sophisticated. Temperature is a key factor influencing the fouling mass through three terms in the model. The highest contribution to fouling mass is provided by the highest temperature located at the PHE outlet. It is then possible to move the deposition formation area into a less sensitive area of the installation without heat exchange wall for example.

The objective of providing a simple general model to predict the fouling situation inside the PHE was achieved for three different whey protein concentrates within the parameters range explored. This may give guidelines for fouling mitigation and control, or in turn, help to understand how and to what extent different anti-fouling solutions function e.g. surface modification of the heat exchanger such as (Zouaghi, Six, Bellayer, Moradi, Hatzikiriakos, Dargent, et al., 2017; Zouaghi, Barry, Bellayer, Lyskawa, André, Delaplace, et al., 2018).

Acknowledgements

This work was supported by the French State and the Hauts-de-France region [CPER ALIBIOTECH program].

References

Awad, M. M. (2011). fouling of heat transfer surfaces. In P. Aziz Belmiloudi (Ed.). *heat transfer - theoretical analysis, experimental investigations and industrial systems*InTech978-953-307-226-5. Available from: http://www.intechopen.com/books/heat-transfer-theoretical-analysis-experimentalinvestigations-and-industrial-systems/fouling-of-heat-transfer-surfaces.

Bansal, B., & Chen, X. D. (2006). A critical review of milk fouling in heat exchangers. *Comprehensive Reviews in Food Science and Food Safety, 5*(2), 27–33.

Belmar-Beiny, M. T., Gotham, S. M., Paterson, W. R., Fryer, P. J., & Pritchard, A. M. (1993). The effect of Reynolds number and fluid temperature in whey protein fouling. *Journal of Food Engineering, 19*(2), 119–139.

Benning, R., Petermeier, H., Delgado, A., Hinrichs, J., Kulozik, U., & Becker, T. (2003). Process design for improved fouling behaviour in dairy heat exchangers using a hybrid modelling approach. *Food and Bioproducts Processing, 81*(3), 266–274.

Blanpain-Avet, P., André, C., Khaldi, M., Bouvier, L., Petit, J., Six, T., et al. (2016). Predicting the distribution of whey protein fouling in a plate heat exchanger using the kinetic parameters of the thermal denaturation reaction of β-lactoglobulin and the bulk temperature profiles. *Journal of Dairy Science, 99*(12), 9611–9630.

Blanpain-Avet, P., Hédoux, A., Guinet, Y., Paccou, L., Petit, J., Six, T., et al. (2012). Analysis by Raman spectroscopy of the conformational structure of whey proteins constituting fouling deposits during the processing in a heat exchanger. *Journal of Food Engineering, 110*(1), 86–94.

Bouvier, L., Moreau, A., Ronse, G., Six, T., Petit, J., & Delaplace, G. (2014). A CFD model as a tool to simulate β-lactoglobulin heat-induced denaturation and aggregation in a plate heat exchanger. *Journal of Food Engineering, 136*, 56–63.

Boxler, C. (2015). *Fouling by milk constituents and cleaning of modified surfaces*Thesis. Technische Universität Braunschweig.

Buckingham, E. (1914). On physically similar systems; Illustrationsof the use of dimensional equations. *Physical Review, 4*, 345–376 New York; 2nd Series 4.

Burton, H. (1968). Deposit of whole milk in treatment plants—a review and discussion. *Journal of Dairy Research, 34*, 317–330.

Bylund, G. (1995). *Dairy processing handbook.* Lund, Sweden: Tetra Pak Processing Systems AB.

Changani, S. D., Belmar-Beiny, M. T., & Fryer, P. J. (1997). Engineering and chemical factors associated with fouling and cleaning in milk processing. *Experimental Thermal and Fluid Science, 14*(4), 392–406.

Daufin, G., Labbé, J. P., Quemerais, A., Brulé, G., Michel, F., Roignant, M., et al. (1987). Fouling of a heat exchange surface by whey, milk and model fluids. An analytical study. *Le Lait, 67*(3), 339–364.

Delaplace, G., Loubière, K., Ducept, F., & Jeantet, R. (2015). *Dimensional analysis of food processes.* ISTE Press, Elsevier9781785480409.

Delplace, F., Leuliet, J. C., & Leviex, D. (1997). A reaction engineering approach to the analysis of fouling by whey proteins of a six-channels-per-pass plate heat exchanger. *Journal of Food Engineering, 34*(1), 91–108.

Delplace, F., Leuliet, J.-C., & Tissier, J. P. (1994). Fouling experiments of a plate heat exchanger by whey proteins solutions. *Transactions of IChemE (Part C), 72*, 163–169.

Fryer, P. J., Christian, G. K., & Liu, W. (2006). How hygiene happens: Physics and chemistry of cleaning. *International Journal of Dairy Technology, 59*(2), 76–84.

Fryer, P. J., Robbins, P. T., Green, C., Schreier, P. J. R., Pritchard, A. M., Hasting, A. P. M., et al. (1996). A statistical model for fouling of a plate heat exchanger by whey protein solution at UHT conditions. *Food and Bioproducts Processing, 74*(4), 189–199.

Georgiadis, M. C., & Macchietto, S. (2000). Dynamic modelling and simulation of plate heat exchangers under milk fouling. *Chemical Engineering Science, 55*(9), 1605–1619.

Georgiadis, M. C., Rotstein, G. E., & Macchietto, S. (1998). Modelling and simulation of complex plate heat exchanger arrangements under milk fouling. *Computers & Chemical Engineering, 22*, S331–S338.

Gotham, S. M., Fryer, P. J., & Pritchard, A. M. (1992). β-Lactoglobulin denaturation and aggregation reactions and fouling deposit formation: A DSC study. *International Journal of Food Science and Technology, 27*(3), 313–327.

Grijspeerdt, K., Mortier, L., De Block, J., & Van Renterghem, R. (2004). Applications of modelling to optimise ultra high temperature milk heat exchangers with respect to fouling. *Food Control, 15*(2), 117–130.

Guérin, R., Ronse, G., Bouvier, L., Debreyne, P., & Delaplace, G. (2007). Structure and rate of growth of whey protein deposit from in situ electrical conductivity during fouling in a plate heat exchanger. *Chemical Engineering Science, 62*(7), 1948–1957.

Havea, P., Singh, H., & Creamer, L. K. (2001). Characterization of heat-induced aggregates of β-lactoglobulin, α-lactalbumin and bovine serum albumin in a whey protein concentrate environment. *Journal of Dairy Research, 68*(3), 483–497.

de Jong, P. (1997). Impact and control of fouling in milk processing. *Trends in Food Science & Technology, 8*(12), 401–405.

Jun, S., & Puri, V. M. (2005a). 3D milk-fouling model of plate heat exchangers using computational fluid dynamics. *International Journal of Dairy Technology, 58*(4), 214–224.

Jun, S., & Puri, V. M. (2005b). Fouling models for heat exchangers in dairy processing: A review. *Journal of Food Process Engineering, 28*(1), 1–34.

Jun, S., & Puri, V. M. (2007). plate heat exchanger: Thermal and fouling analysis. In D.-W. Sun (Ed.). *Computational fluid dynamics in food processing* (pp. 417–430). New York: CRC Press.

Khaldi, M., Blanpain-Avet, P., Guérin, R., Ronse, G., Bouvier, L., André, C., et al. (2015). Effect of calcium content and flow regime on whey protein fouling and cleaning in a plate heat exchanger. *Journal of Food Engineering, 147*, 68–78.

Khaldi, M., Croguennec, T., André, C., Ronse, G., Jimenez, M., Bellayer, S., et al. (2018). Effect of the calcium/protein molar ratio on β-lactoglobulin denaturation kinetics and fouling phenomena. *International Dairy Journal, 78*, 1–10.

Khaldi, M., Ronse, G., André, C., Blanpain-Avet, P., Bouvier, L., Six, T., et al. (2015). Denaturation kinetics of whey protein isolate solutions and fouling mass distribution in a plate heat exchanger. *International Journal of Chemical Engineering, 2015*, 10. Article ID 139638 https://doi.org/10.1155/2015/139638.

Kroslak, M., Sefcik, J., & Morbidelli, M. (2007). Effects of temperature, pH, and salt concentration on β-lactoglobulin deposition kinetics studied by optical waveguide lightmode spectroscopy. *Biomacromolecules, 8*(3), 963–970.

Lalande, M., & Tissier, J.-P. (1985). Fouling of heat transfer surfaces related to β-lactoglobulin denaturation during heat processing of milk. *Biotechnology Progress, 1*(2), 131–139.

Lyster, R. L. J. (1970). The denaturation of α-lactalbumin and β-lactoglobulin in heated milk. *Journal of Dairy Research, 37*(2), 233–243.

Lyster, R. L. J. (2009). The composition of milk deposits in an ultra-high-temperature plant. *Journal of Dairy Research, 32*(2), 203–208.

Mahdi, Y., Mouheb, A., & Oufer, L. (2009). A dynamic model for milk fouling in a plate heat exchanger. *Applied Mathematical Modelling, 33*(2), 648–662.

Mota, F. A. S., Carvalho, E. P., & Ravagnani, M. A. S. S. (2015). Modeling and design of plate heat exchanger. In S. N. Kazi (Ed.). *Heat transfer studies and applications*Rijeka: InTech pp. Ch. 07.

Nicolai, T., Britten, M., & Schmitt, C. (2011). β-Lactoglobulin and WPI aggregates: Formation, structure and applications. *Food Hydrocolloids, 25*(8), 1945–1962.

Pan, F., Chen, X. D., Mercadé-Prieto, R., & Xiao, J. (2019). Numerical simulation of milk fouling: Taking fouling layer domain and localized surface reaction kinetics into account. *Chemical Engineering Science, 197*, 306–319.

Petit, J., Herbig, A. L., Moreau, A., & Delaplace, G. (2011). Influence of calcium on β-lactoglobulin denaturation kinetics: Implications in unfolding and aggregation mechanisms. *Journal of Dairy Science, 94*(12), 5794–5810.

Petit, J., Six, T., Moreau, A., Ronse, G., & Delaplace, G. (2013). β-lactoglobulin denaturation, aggregation, and fouling in a plate heat exchanger: Pilot-scale experiments and dimensional analysis. *Chemical Engineering Science, 101*, 432–450.

René, F., & Lalande, M. (1988). Descriptions et mesures des phénomènes d'encrassement des échangeurs de chaleur. Cas du traitement thermique du lait. *Entropie, 139*, 13–23.

Sadeghinezhad, E., Kazi, S. N., Dahari, M., Safaei, M. R., Sadri, R., & Badarudin, A. (2015). A comprehensive review of milk fouling on heated surfaces. *Critical Reviews in Food Science and Nutrition, 55*(12), 1724–1743.

Sherwin, C. P., & Foegeding, E. A. (1997). The effects of $CaCl_2$ on aggregation of whey proteins. *Milchwissenschaft, 52*, 93–96.

Szirtes, T. (1998). *Applied dimensional analysis and modeling.* New York: McGraw-Hill.

Tolkach, A., & Kulozik, U. (2007). Reaction kinetic pathway of reversible and irreversible thermal denaturation of β-lactoglobulin. *Dairy Science & Technology, 87*, 301–315.

Truong, T. H., Kirkpatrick, K., & Anema, S. G. (2017). Role of β-lactoglobulin in the fouling of stainless steel surfaces by heated milk. *International Dairy Journal, 66*, 18–26.

Zlokarnik, M. (2002). *Scale-up in chemical engineering.* Weinheim: Wiley-VCH.

Zouaghi, S., Barry, M. E., Bellayer, S., Lyskawa, J., André, C., Delaplace, G., et al. (2018). Antifouling amphiphilic silicone coatings for dairy fouling mitigation on stainless steel. *Biofouling, 34*(7), 769–783.

Zouaghi, S., Frémiot, J., André, C., Grunlan, M. A., Gruescu, C., Delaplace, G., et al. (2019). Investigating the effect of an antifouling surface modification on the environmental impact of a pasteurization process: An LCA study. *ACS Sustainable Chemistry & Engineering, 710*, 9133–9142.

Zouaghi, S., Six, T., Bellayer, S., Moradi, S., Hatzikiriakos, S. G., Dargent, T., et al. (2017). Antifouling biomimetic liquid-infused stainless steel: Application to dairy industrial processing. *ACS Applied Materials & Interfaces, 9*(31), 26565–26573.